International Journal of Environmental Research and Public Health

MDPI

Article

Lipid biomarker investigation of delivery and preservation of autochthonous organic carbon in the Pearl River and their contribution to carbon sink: Evidence from the water and surface sediment

Mingxing Yang [1], Zaihua Liu [2,*], Hailong Sun [2], Min Zhao [2] and Haibo He [2]

[1] Faculty of Resources and Environmental Engineering, Guizhou Institute of Technology, Guiyang 550003, China; yangmingxing@git.edu.cn
[2] State Key Laboratory of Environmental Geochemistry, Institute of Geochemistry, Chinese Academy of Sciences, Guiyang 550081, China; sunhailong@vip.gyig.ac.cn (H.S.); zhaomin@mail.gyig.ac.cn (M.Z.); hehaibo@mail.gyig.ac.cn (H.H.)
* Correspondence: liuzaihua@vip.gyig.ac.cn

Abstract: The molecular compositions of lipid biomarkers in surface water, the water column and surface sediments collected along the Pearl River were investigated to identify the delivery and preservation of autochthonous organic carbon (AOC) and to estimate its contribution to carbon sink. Spatial distribution of lipid biomarkers showed that samples collected at the high DIC (dissolved inorganic carbon) concentration sites had prominent aquatic autochthonous signatures, while samples collected at the low DIC concentration sites showed greater terrestrial contributions, which was described as the DIC fertilization effects. In the summer, there was typically intense precipitation and flood erosion that diluted the biogeochemical composition and carried terrestrial plant detritus. Therefore, the percentage of AOC (auto%) was higher in winter than in summer. According to the calculation of lipid biomarkers, the values of auto% were 65% (winter) and 54% (summer) in surface water, 55.9% (winter) and 44.6% (summer) in below surface water, and 52.1% (winter) and 43.9% (summer) in surface sediment, which demonstrated that AOC accounted for a major part of the TOC. Vertical variability mainly appeared at sites with intense flood erosion that resulted in the mixing and deposition of resuspended sediments. There is a positive correlation of clay content with the auto% value and the biogeochemical composition, reflecting that clay adsorbed organic carbon in the water, vertically deposited it into the sediment, and was the dominant mechanism of vertical delivery of organic carbon (OC). According to the new karst carbon sink model, based on coupled carbonate weathering and aquatic photosynthesis, the karst carbon sink flux (CSF) in Pearl River was 2.69×10^6 t/a, which was 1.7 times traditional estimation (1.58×10^6 t/a), which didn't consider formation of AOC. This indicates that the contribution of the riverine system to global karst carbon sink may have been highly underestimated before.

Keywords: Biological carbon pump; Autochthonous organic carbon; Aquatic photosynthesis; Carbonate weathering; Karst carbon sink flux; Pearl River Basin

Citation: Wu, Y.; Min, Z.; Mingxing, Y.; Jun, Y. Exploration on the Implementation of Carbon Neutralization in the Field of Natural Resources under the Background of Sustainable Development—An Overview. *Environ. Res. Public Health* **2022**, *19*, x. https://doi.org/10.3390/xxxxx

Academic Editor: Firstname Lastname

Received: date
Accepted: date
Published: date

Publisher's Note: MDPI stays neutral with regard to jurisdictional claims in published maps and institutional affiliations.

Copyright: © 2022 by the authors. Submitted for possible open access publication under the terms and conditions of the Creative Commons Attribution (CC BY) license (https://creativecommons.org/licenses/by/4.0/).

1. Introduction

The biological carbon pump (BCP) is a process that convert atmosphere CO2 into recalcitrant organic carbon through the photosynthesis and microbial action. Usually, BCP can be divided into three distinct phases. The first phase is the fixation of atmospheric CO_2 into dissolved inorganic carbon (DIC: CO_2(aq), HCO_3^- and CO_3^{2-}), which occurs at the interface between the atmosphere and the surface of the water [1, 2]. Following the first

phase, phytoplankton in the aquatic system uses DIC during photosynthesis to make organic carbon (including lipids, carbohydrates, and proteins) [3-6]. Finally, organic carbon is transported into the ocean by flowing river water or adsorbed by suspended particle matter and deposited into the sediment [7, 8].

Due to the BCP effect, the OC transformed from DIC by aquatic photosynthesis is called autochthonous organic carbon and is derived from phytoplankton (mainly algae), which is a significant part for river carbon storage [9, 10]. On the other hand, the OC derived from degradation products of higher plants is called allochthonous OC [11].

It is obvious that the BCP effect is an important sequestered carbon process. Especially in karst basins, the rapid carbonate weathering can offer sufficient DIC as carbon source for aquatic photosynthesis, the amount of autochthonous OC can be considerable, therefore, its contribution to karst-related carbon sinks must be take into account [12, 13]. However, because of autochthonous and allochthonous OCs are mixed together in the aquatic system, it is difficult to quantify the ratios of autochthonous and allochthonous. Moreover, autochthonous OC is regarded as part of allochthonous OC and the total amount of carbonate weathering-coupled-photosynthesis carbon sink is greatly underestimated. Hence, the primary task for carbon sink assessment in the aquatic system is to distinguish the autochthonous and allochthonous OCs.

Another important factor of the carbon cycle in the riverine system is the vertical delivery and preservation of organic carbon, because more than 80% of it is buried in coastal marine systems adjacent to rivers [14-17]. Usually, the OC is transported with inorganic clasts [18] or as discrete OC particles. Globally, OC in the suspended particle and sediment is thought to be largely associated with clay content (＜2μm, %) [19]. Furthermore, OC may have a high affinity for clay surfaces rather than for any mineral surfaces [20-23]. Finally, clay particles can comprise a significant component of TOC from the water column to sediment [24]. Despite the global significance of TOC delivery from large rivers to the ocean, the vertical diversity and amount of TOC in these settings are still poorly understood.

Hence, the assessment of karst-related carbon sinks in the riverine system is still imprecise. There are two obstacles in addressing this problem: 1) material transportation in the riverine system is a complex process in terms of erosion, sediment, weathering, etc., which leads to difficulty in distinguishing the autochthonous and allochthonous OC; 2) vertical delivery of OC is neglected, and thus the amount of carbon sink may be dramatically underestimated.

Lipid compounds (also known as molecular fossils) are derived from dead biological residues, which preserved the carbon skeleton of the original biochemical component and recorded the relevant information of the original biological parent material, can be used to identify their sources [25, 26]. It has been reported that aquatic organisms usually produce short to mid-chain n-alkanes. Inversely, terrigenous higher plants usually produce long chain n-alkanes [27-29]. Monounsaturated fatty acids (MUFA) (e. g. C16:1ω and C18:1ω) are used to represent fresh algal sources [30]. Higher plant sources of Polyunsaturated fatty acids (PUFA) (e. g. C18:2ω and C18:3ω) are used to represent higher plant sources[31]. Besides, sitosterol ($29^{\Delta5}$) and campesterol ($28^{\Delta5}$) sterols are biomarkers of terrestrial plants while epi-brassicasterol ($28^{\Delta5,22}$) is particularly found in phytoplankton[32]. Another phytoplanktonic marker, 24-methylenecholesterol ($28^{\Delta5,24}$) is characteristic of diatoms [32]. Therefore, lipid biomarkers were widely used to distinguish OC sources [33, 34].

Previous studies have examined the contribution of riverine water to the carbon sink through carbonate weathering coupled with aquatic photosynthesis. However, concerns on the vertical delivery and preservation of AOC in big rivers have not fully been understood. It is of great importance to take the big rivers into account when the carbon balance is researched at the global level. The Pearl River, the third largest river of China, is characterized by its typical carbonate cover and large amount loading of sediment, offering a perfect location for the carbonate weathering coupled-photosynthesis carbon sink study.

In this work, we follow the seasonal and spatial transportation and conversion of DIC and OC during the BCP process with chemical, lipid biomarkers and phytoplankton analysis in both water column and sediments of the Pearl River to achieve the following: 1) describe the seasonal variations of geochemical and lipid biomarkers in both the water column and sediments in the Pearl River; 2) examine the vertical distribution of the autochthonous OC based on the BCP effect; and 3) estimate the amount of autochthonous OC in the Pearl River.

2. Materials and Methods

2.1. Study area and sampling sites

2.1.1. Study area

The Pearl River originates in the Wumeng Mountains in the western Yunnan Province, flows east and empties into the South China Sea [33]. Xijiang, Beijiang and Dongjiang are the main tributaries of Pearl River (Figure 1). Xijiang is the largest tributary and is located in the upper and middle reaches of Pearl River basin [36]. The upper reach includes two large tributaries, Nanpanjiang and Beipanjiang (first order tributaries of Xijiang). The middle reach includes the large tributaries of Liujang, Guijiang and Yujiang (first order tributaries of Xijiang). The lower reach includes the Beijiang and Dongjiang tributaries (Figure 1). The Pearl River basin is dominated by a subtropical to tropical monsoon climate. From east to west, the mean annual temperature and precipitation across the basin ranges from 14 ℃ to 22 ℃ and 1200 mm to 2200 mm, respectively [37].

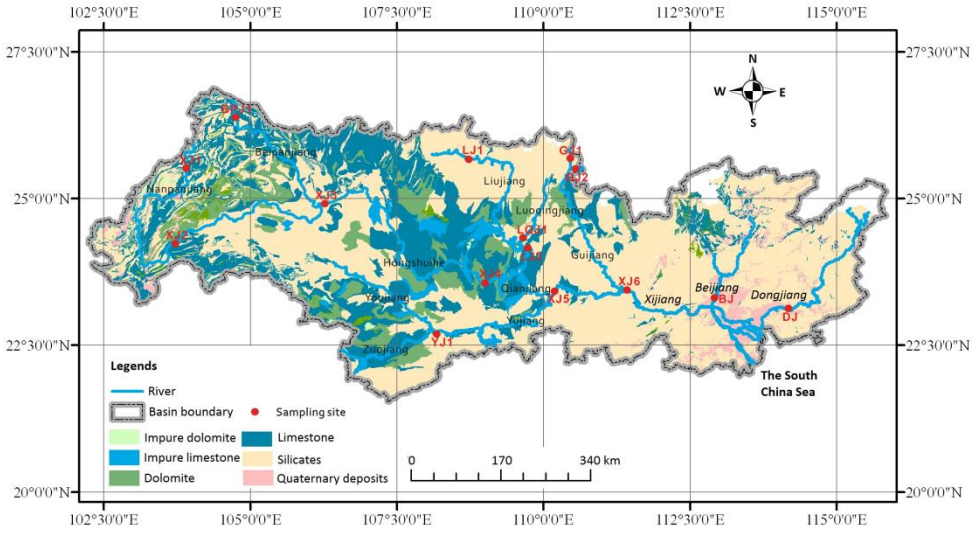


Figure 1. Geology of the Pearl River and sampling sites.

The annual average runoff and sediment load of Pearl River from 1954 to 2010 of the entire basin were 283×10^9 m^3 and 72.4×10^6 t, respectively [38]. From April to September, the accumulative runoff and sediment load account for 84% and 94% of the annual totals. During the flood season, the runoff and sediment load account for 50% and 72% of the annual totals [39]. In geographical and geological senses, Pearl River basin is characterized with widely carbonate rocks distribution (especially in the upper and middle reaches, which account for approximately 45% of the basin, Figure 1). Besides, Clastic rock and graniteis are mainly located in the upper reach (approximately 27% of the basin) and lower reach (approximately 16% of the basin), respectively [40].

2.1.2. Sample collection

In order to contrast the different climate impacts, we collected water samples at 5 cm below the water surface in winter (dry season) and summer (wet season), respectively. All

the sampling locations were represent the Pearl River and its main distributaries in terms of lithological, climatic and hydrological impacts (Table 1). Vertical water samples were collected in six sections (XJ2, XJ3, XJ4, XJ6, BJ and DJ) at five depths (0 m, 2 m, 4 m, 6 m and 8 m). Among those sections, XJ2, XJ3, XJ4, XJ6 represent the Xijiang River and BJ and DJ represent the Beijiang River and Dongjiang River, respectively.

Table 1. Description of sampling sites.

Site	Location	Tributary description	Sample types			TSS* (mg/L)	T* (℃)	Precipitation* (mm/a)
			Surface water	Column water	Sediment			
XJ1	25° 36′ 18″ N; 103° 49′ 33″ E	Upstream of Nanpanjiang	√			1290	18.6	1000.0
XJ2	24° 01′ 13″ N; 103° 36′ 20″ E	Midstream of Nanpanjiang	√	√	√	680	20.2	963.7
BPJ1	26° 29′ 59″ N; 103° 44′ 07″ E	Upstream of Beipanjiang	√			2610	18.7	1127.6
XJ3	24° 57′ 47″ N; 106° 08′ 55″ E	Junction of Nanpanjiang and Beipanjiang	√	√	√	170	19.1	921.1
XJ4	23° 44′ 04″ N; 109° 13′ 43″ E	Downstream of Hongshuihe	√	√	√	628	20.8	1499.8
YJ1	22° 48′ 38″ N; 108° 18′ 46″ E	Junction of Zuojiang and Youjiang	√			241	21.6	1304.2
LQJ1	24° 24′ 09″ N; 109° 36′ 25″ E	Downstream of Luoqingjiang	√			132	20.0	1257.7
LJ1	25° 13′ 07″ N; 109° 23′ 47″ E	Upstream of Liujiang	√			143	19.0	1493.0
LJ2	24° 14′ 36″ N; 109° 43′ 13″ E	Junction of Liujiang and Luoqingjiang	√			132	21.6	1304.2
XJ5	23° 27′ 50″ N; 110° 09′ 39″ E	Junction of Qianjiang and Yujiang	√			350	21.4	1726.7
GJ1	25° 31′ 17″ N; 110° 11′ 41″ E	Upstream of Guijiang	√			67	18.0	2052.0
GJ2	25° 06′ 19″ N; 110° 24′ 55″ E	Upstream of Guijiang	√			92	18.7	1926.0
XJ6	23° 28′ 40″ N; 111° 17′ 11″ E	Downstream of Xijiang	√	√	√	311	21.1	1503.6
BJ	23° 41′ 21″ N; 113° 03′ 26″ E	Downstream of Beijiang	√	√	√	129	20.7	1900.1
DJ	23° 09′ 28″ N; 114° 16′ 12″ E	Downstream of Dongjiang	√	√	√	107	22.1	1821.2

* annual mean value.

500mL of water was collected in a brown bottle at each site for GC–MS analysis (types and concentrations of OCs). Water temperature (T), pH, dissolved oxygen (DO), and electrical conductivity (EC) of water samples were measured by the WTW Technology Multi-Line 350i. All the meters were calibrated before use. Besides, another bottle of 500mL water was added 1% $MgCO_3$ and Lugol's solution to determine Chlorophyll a (Chl a) and biomass. Sediments (0~5 cm of the riverbed) six sections (shown in table 1) were grabbed as samples.

2.2. Chemical analysis

Merck field test boxes were applied to measure HCO_3^- and Ca^{2+} in water samples[41]. Anion and cation concentrations were measured by ion chromatograph (ICS–90, Dionex)

and ICP–OES (Vista MPX, Varian, USA), respectively. The pCO_2 (CO_2 partial pressure) and SIc (calcite saturation index) were calculated using the WATSPECT program [42]. Blood counting chamber was used to determine the amount of biomass in water sample. A UV spectrophotometer was used to measure the OD680 and turbidity of water samples according to the handbook of Monitoring and Analysis Method of Water and Waste Water [43].

Chl a was extracted from water samples by using a 90% acetone solution before analysis. After supersonic treatment, the extracts were measured with a UV spectrophotometer and the Chl a concentration was determined according to standard methods established by the Ministry of Environmental Protection of China [43].

2.3. Biomarker analysis

MeOH and hexane were used to extract the organic compounds in water samples. All the extracted substance were then condensed to 1 mL by the rotary evaporater. A portion of the extract was saponified using 1 M KOH in aqueous MeOH. Neutral and acidic lipids were extracted into hexane from the saponified sample. Fatty acids were converted to methyl esters using BF3–MeOH. Both fatty acids and neutral lipids were separated from other lipid classes by silica gel chromatography. Sterols were derivatized to trimethylsilyl ethers using BSTFA in acetonitrile and heating at 70 °C for 30 min [9]. Lipid biomarkers in sediment samples (3.0 g, dry weight) were extracted in a Soxhlet apparatus with 210 mL of a mixture of dichloromethane and methanol (2:1, v:v) for 20 h. Subsequent processes were similar for the water samples.

A gas chromatography (GC) (Agilent 7890A) was used to measure fatty acid, sterols and n-alkanes. The size of column was 30 m×0.32 mm×0.25 μm (item: DB5). The qualitative analysis of organic compounds were determined by comparing the retention time of the external standards (Sigma–Aldrich Company).

Meanwhile, the concentrations of compounds were measured by calculating their total ion current (TIC) peak area. GC-MS running program of each types of compound were: (1)Fatty acids, the initial temperature was 60 °C, then increased to 150 °C with the rate of 40 °C/min. Then, increased from the 150 °C to 240 °C with the rate of 3 °C/min and was kept for 15 min. (2)Sterols, raised the temperature from 80 °C (kept for 1 min) to 200 °C with the rate of 25 °C/min, and then raised from 200 °C to 250 °C with the rate of 3 °C/min and subsequently increase to 300 °C (rate: 1.8 °C/min, kept for 2 min). (3)n-alkanes, the temperature was held at 70 °C for 1 min, then raised to 140 °C with the rate of 10 °C/min, and subsequently increased by 3 °C/min to 310 °C and held for 15 min [44].

2.4. Grain size of suspended sediment and TSS analysis

All surface sediment and core samples were pretreated with 10 – 20 ml of 30% H_2O_2 to remove organic matter, washed with 10% HCl to remove carbonates and mollusk fragments, rinsed with deionized water, and then placed in an ultrasonic vibrator for several minutes to facilitate dispersion. Then, a Malvern Mastersizer 2000 grain size analyzer was used to measure the grain size of both sediments and TSS.

3. Results

3.1. Seasonal variation of chemical, phytoplankton and biomarker compositions and their implication for coupled carbonate weathering with aquatic photosynthesis

3.1.1. Seasonal distribution of biochemical compositions in surface water and the DIC fertilization effect

(1) Chemical composition

Chemical composition of the water during the winter (dry season) and summer (wet season) in terms of HCO_3^-, Ca^{2+}, pCO_2, pH and EC is shown in Figure 2. HCO_3^- is the major

part of DIC; its spatial and seasonal distribution in the Pearl River was quite varied. Overall, sites with a primarily carbonate bedrock offered an abundant DIC source. XJ1, for example, had a DIC concentrations of 4.6 mmol/L and 3.5 mmol/L in winter and summer, respectively, whereas the lowest value appeared at the silicate area, GJ1 (upper Guijiang) with DIC concentrations of 0.4 mmol/L and 0.5 mmol/L. There was a great difference of HCO_3^- concentration between the karst area and the non-karst area. The same pattern were found in the Ca^{2+} concentration. Morespecifically, Ca^{2+} concentration ranged from 88.0 mg/L (XJ1) to 10.0 mg/L (GJ1) in winter (average 46.9 mg/L) and 60.0 mg/L (XJ1) to 8.0 mg/L (GJ1) in summer (average 33.9 mg/L).

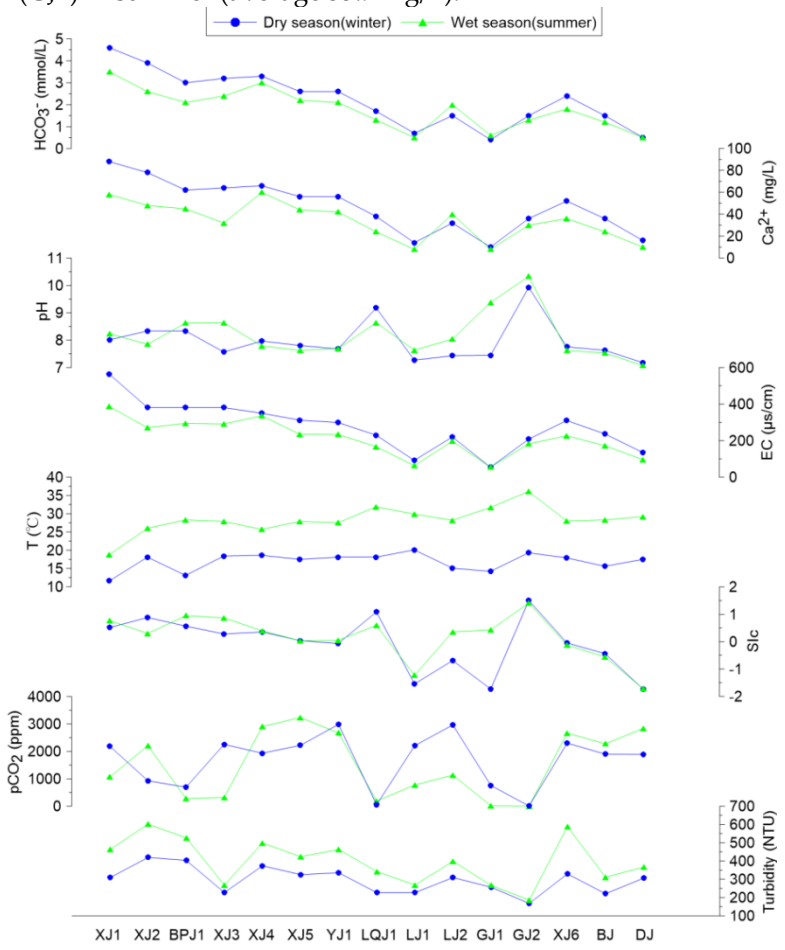


Figure 2. Geochemical parameters of water samples in the Pearl River basin.

The pCO_2 value ranged from 4.1 ppm to 2985.0 ppm (average 1684.0 ppm) in winter and 0.4 ppm to 3235.9 ppm (average 1503.9 ppm) in summer. The SIc value ranged from -1.73 to 1.52 (average -0.07) in winter and -1.72 to 1.41 (average 0.17) in summer.

(2) Phytoplankton composition

Due to the BCP effect, the DIC (mainly HCO_3^-) is utilized during photosynthesis in the aquatic ecosystem. The products include OC and phytoplankton, especially algae. Therefore, the features of phytoplankton and their relation with DIC distribution were of great importance for understanding the mechanism of the BCP effect.

The average concentration of Chl a in winter and summer was 6.3 mg/m^3 and 8.6 mg/m^3, respectively, showing that photosynthesis in summer was more intense than winter [45]. Apart from the in situ aquatic photosynthesis, terrestrial flushing materials could also carry Chl a into inland water.

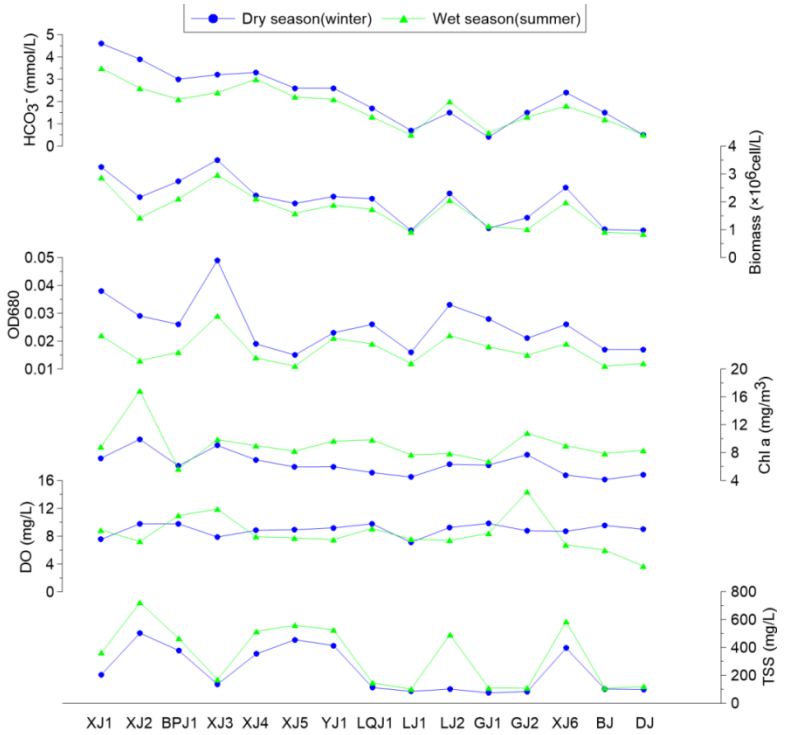


Figure 3. Characteristics of Phytoplankton in water samples in the Pearl River basin.

Another product of photosynthesis in aquatic system is the accumulation of biomass (mainly phytoplankton, such as algae). The average phytoplankton biomass was 2.0×10^6 cell/L and 1.7×10^6 cell/L in winter and summer, respectively. The highest phytoplankton biomass (3.5×10^6 cell/L in winter and 2.9×10^6 cell/L in summer) was detected at XJ3 (where the DIC concentration was high, water flow was low and the concentration of TSS was low), which offered the photosynthesis with large amounts of DIC and stable environment. Inversely, with low DIC and high water flow, photosynthesis was weaker at DJ, which caused the low biomass (1.0×10^6 cell/L in winter and 0.9×10^6 cell/L in summer).

The OD680 values exhibited the same trend with biomass. These statistical correlation illustrated that phytoplankton were more intense at the upstream sites (high DIC concentrations). However, phytoplankton at the downstream sites (low DIC concentrations) also slightly proceed and offered biomass in the aquatic system (Figure. 3).

3.1.2. Biomarkers distribution in surface water -- implication for coupled carbonate weathering with aquatic photosynthesis

Lipid biomarkers in terms of fatty acids, sterols and n-alkanes in surface water were measured and are listed in Table 2 to demonstrate their implication for source appointment between aquatic and terrigenous organic carbon.

Table 2. Biomarkers at various sites in Pearl River and their relevant values.

Site	Fatty acids				Sterols			n-Alkanes		
	SSFA (%)	BSFA (%)	MUFA (%)	PUFA (%)	$28\Delta^{5,22}$ (μg/L)	$29\Delta^5$ (μg/L)	$27\Delta^5/29\Delta^{5,22}$ $+29\Delta^5$	TAR_{HC}	CPI_{HC}	C17 (μg/L)
XJ1	72.0/63.2	2.2/9.6	19.7/10.6	6.1/16.6	1.2/0.7	0.2/0.4	4.79/3.56	0.38/0.46	1.56/2.01	296.3/208.6
XJ2	66.5/49.6	8.3/18.2	17.5/12.6	7.7/19.6	1.5/0.8	0.4/1.1	4.32/3.12	0.61/0.72	2.09/3.06	255.3/158.8
BPJ1	60.3/52.2	8.411.5/	16.5/13.9	14.7/22.4	0.9/0.6	0.2/0.5	3.53/3.11	0.55/0.61	2.12/2.49	266.3/188.5
XJ3	61.2/58.3	4.1/5.1	23.8/21.6	10.8/15.0	1.7/1.5	0.1/0.2	7.29/6.89	0.26/0.29	1.18/1.61	311.2/278.5
XJ4	65.4/55.6	3.8/14.7	19.2/15.2	11.6/14.5	0.9/0.6	0.2/0.6	3.90/3.01	0.47/0.51	2.92/4.03	216.3/156.6
YJ1	53.5/49.0	10.8/22.1	13.7/10.8	22.1/24.7	1.5/1.1	0.2/0.7	1.89/1.68	0.59/0.61	3.43/3.98	243.2/146.3
LQJ1	62.9/64.8	12.7/16.8	6.6/5.1	17.8/13.3	1.1/0.6	0.3/0.4	2.79/2.81	0.61/0.73	3.79/4.28	163.2/112.6

LJ1	55.0/58.9	21.7/24.8	10.0/5.5	13.4/10.8	0.4/0.4	0.2/0.8	1.45/1.22	0.48/0.41	2.28/3.56	35.6/31.1
LJ2	77.1/73.9	3.7/9.7	14.8/15.3	4.4/1.1	0.4/0.5	0.2/0.4	0.81/0.89	0.52/0.58	4.99/5.01	35.6/28.2
XJ5	62.2/64.9	4.8/8.9	12.8/14.2	20.1/12.0	0.6/0.6	0.3/0.3	2.02/2.88	0.52/0.66	2.88/2.58	189.0/136.1
GJ1	62.7/58.2	17.2/19.5	8.7/13.2	11.4/9.1	0.4/0.4	0.2/0.4	0.67/0.56	0.49/0.51	3.32/2.96	47.7/61.9
GJ2	63.3/70.1	16.5/15.8	7.2/9.8	13.0/4.3	0.7/0.9	0.2/0.4	1.59/1.41	0.46/0.55	3.52/4.12	69.9/72.8
XJ6	58.6/53.3	12.2/15.2	15.6/8.5	13.6/23.0	1.3/0.6	0.3/0.5	1.99/1.58	0.51/0.62	2.33/2.80	68.0/50.1
BJ	72.5/68.2	6.4/10.2	11.7/11.3	9.5/10.3	0.9/0.5	0.4/0.5	0.89/0.93	0.68/0.75	4.71/5.06	88.8/68.3
DJ	63.9/53.6	10.1/16.0	9.9/10.1	16.0/20.5	0.3/0.4	0.4/0.6	1.11/1.21	0.72/0.81	3.16/4.88	45.2/39.8
mean	63.8/59.6	9.5/14.1	13.9/11.8	12.8/14.5	0.9/0.7	0.3/0.5	2.60/2.32	0.52/0.58	2.99/3.49	149.3/115.8

Data before and after "/" represented winter and summer results, respectively; SSFA (straight saturated fatty acids), BSFA (branched saturated fatty acids); TAR_{HC}=(C27+C29+C31)/(C15+C17+C19); CPI_{HC}=0.5[(C25 + C27 + C29 + C31 + C33/C24 + C26 + C28 + C30 + C32)+(C25 + C27 + C29 + C31 + C33/C26 + C28 + C30 + C32 + C34)]; C17: Heptadecane.

(1) Fatty acids

In winter, concentrations of the total fatty acid (TFA) were ranged from 11.4 μg/L to 311.8 μg/L with an average of 75.9 μg/L, while in summer ranged from 126.8 μg/L to 689.1 μg/L in summer with an average of 255.6 μg/L. XJ2 and GJ1 represented the highest and lowest values respectively. The TFA concentrations varied with those of HCO_3^-, from 129.7 μg/L (ranging from 62.7 μg/L to 311.8 μg/L) in winter and 488.1 μg/L (ranging from 316.2 μg/L to 689.1 μg/L) in summer at sites with high HCO_3^- concentrations to 35.1 μg/L (ranging from 11.4 μg/L to 56.1 μg/L) in winter and 219.6 μg/L (ranging from 126.8 μg/L to 406.9 μg/L) in summer at sites with low HCO_3^- concentrations. Saturated fatty acids were divided into straight and branched saturated fatty acids (SSFA and BSFA). SSFA, the most abundant class was predominated over long-chain saturated fatty acids, accounting for 63.8% (winter) and 59.6% (summer) of the TFAs. Unsaturated fatty acids were divided into MUFA and PUFA, which can indicate the diatom growth process in the aquatic systems and have been used to determine the autochthonous OCs [46]. The mean percentages of MUFA were 13.2% (winter) and 11.8% (summer), whereas those of PUFA and BSFA were 13.1% (winter) and 11.8% (summer), and 9.9% (winter) and 14.1% (summer) of the TFA, respectively (Table 2). C16:0 (palmitic acid) was the most abundant compound, which accounted for an average of 20.0% of the TFA. C16:1ω (palmitoleic acid) was the major MUFA and used to indicate autochthonous production. Water samples at XJ3 contained the most abundant C16:1ω (23.5 μg/L), whereas DJ had the lowest value (3.6 μg/L). In summer, the concentration of C16:1ω at XJ3 and DJ were 19.8 μg/L and 6.2 μg/L, respectively, illustrated diversity of different sites. The presence of C16:1ω indicated that the photosynthesis of phytoplankton was intense in the Pearl River [47]. Inversely, fluvial erosion in river carried degradation products of terrestrial plants, for example, C18:2ω (linoleic acid), hence to indicate the allochthonous source. The concentration of C18:2ω was between 0.2 μg/L to 17.9 μg/L in winter and 8.9 μg/L to 41.1 μg/L in summer.

(2) Sterols

Concentrations of total sterols ranged from 1.1 μg/L to 3.6 μg/L (average: 2.4 μg/L, winter) and 2.6 μg/L to 5.1 μg/L (average: 3.8 μg/L, summer). $28^{\Delta5,22}$ was the most abundant sterol at all sites, which varied from 0.3 μg/L to 1.7μg/L (winter) and 0.2 μg/L to 1.3μg/L (summer). The highest concentration of $28^{\Delta5,22}$ was detected in the upstream major tributaries (XJ3), which was dominated mainly by carbonate rocks (Figure 1). By contrast, the lowest concentration was observed at DJ, which was dominated by silicate rock (Figure 1). Cholest-5-en-3β-ol ($27^{\Delta5}$) had the same distribution pattern with $28^{\Delta5,22}$, and its average values were 0.8 μg/L (winter) and 0.5 μg/L (summer). $28^{\Delta5}$ and $29^{\Delta5,22}$ were biomarkers for sources of terrestrial plant [48]. Their concentrations in the Pearl River ranged from 0.2 μg/L to 0.8 μg/L (winter); 0.6 μg/L to 1.9 μg/L (summer); and 0.1 μg/L to 0.4 μg/L (winter); 0.5 μg/L to 2.1 μg/L (summer), respectively. Contrary to $28\Delta^{5,22}$ and $27^{\Delta5}$, $28^{\Delta5}$ and $29^{\Delta5,22}$ were found to be enriched at downstream sites where various materials were drained.

(3) n-Alkanes

In winter, the concentration of n-Alkanes was between 601.3 μg/L to 2316.5 μg/L with the average of 1311.8 μg/L. While in summer, it ranged from 881.6 μg/L to 2115.2 μg/L with the average of 1522.1 μg/L in summer. Carbon chain number of n-Alkanes was from C12 to C34 and the abundant compound was C17 (35.6 μg/L to 311.2 μg/L; average, 149.3 μg/L in winter and 28.2 μg/L to 278.5 μg/L; average, 115.8 μg/L in summer). The value of CPI_{HC} were 2.99 and 3.49 on average and ranged from 1.18 to 4.99 (winter) and 1.61 to 5.06 (summer) (Table 2). Upstream tributaries showed the highest value of CPI_{HC}. TAR_{HC} represents the terrestrial-to-aquatic ratio, which was used to evaluate the relative proportions of autochthonous and allochthonous hydrocarbons in aquatic system [49]. The value of TAR_{HC} in the water sample was between 0.26 to 0.63 and 0.29 to 0.81 with average values of 0.52 and 0.58 in winter and summer, respectively.

By combining the distribution of biochemical composition and lipid biomarkers, a positive correlation was found between DIC concentration and the growth of aquatic biomass and autochthonous and specific parameters (C16:1ω/C18:2ω), which reveals that high DIC concentration in the aquatic system could offer more carbon for the photosynthesis process, hence deriving more phytoplankton biomass and forming more autochthonous OC. This phenomenon was reported as the DIC fertilization effect (Figure 4).

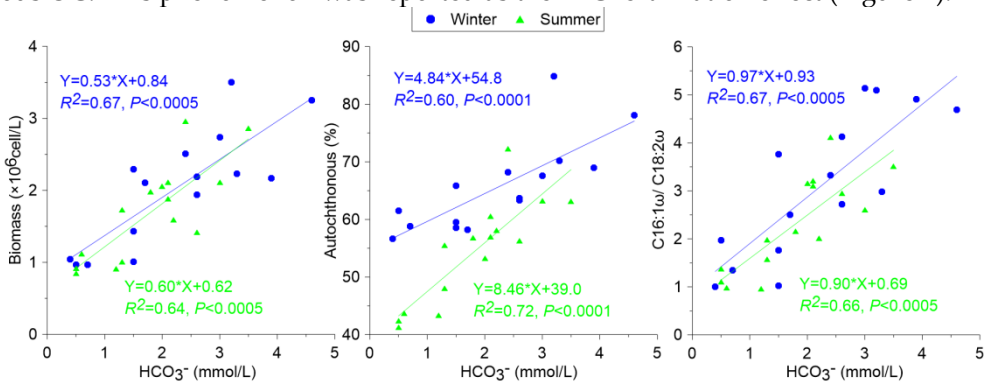


Figure 4. Relationship between photosynthesis and carbon-weathering.

By combining the distribution of biochemical composition and lipid biomarkers, a positive correlation was found between DIC concentration and the growth of aquatic biomass and autochthonous and specific parameters (C16:1ω/C18:2ω), which reveals that high DIC concentration in the aquatic system could offer more carbon for the photosynthesis process, hence deriving more phytoplankton biomass and forming more autochthonous OC. This phenomenon was reported as the DIC fertilization effect (Figure 4).

3.2. Spatial patterns of biomarkers in water column and surface sediments as a consequence of BCP effects

3.2.1. Distribution of lipid biomarkers in water column and surface sediments

Table 3 shows the lipid biomarkers of water column and surface sediment samples from six main sites in the Pearl River. By comparing with the surface water conditions, the vertical distribution also had the same seasonal patterns as discussed above. Variations mainly came from the complex processes during the formation and transportation of autochthonous and allochthonous OC.

Table 3. Lipid biomarker distribution in water column and surface sediment of Pearl River in seasons of winter (W) and summer (S), respectively.

Site	Depth (m)	Fatty acids								Sterols				n-alkanes					
		SSFA (%)		BSFA (%)		MUFA (%)		PUFA (%)		$28\Delta^{5,22}$ (μg/L)		$29\Delta^{5}$ (μg/L)		$27\Delta^{5}/29\Delta^{5,22}$ +$29\Delta^{5}$		TAR_{HC}		CPI_{HC}		C17 (μg/L)	
		W	S	W	S	W	S	W	S	W	S	W	S	W	S	W	S	W	S	W	S

XJ2	0	66.5	49.6	8.3	18.2	17.5	12.6	7.7	19.6	1.5	0.8	0.4	1.1	4.32	3.12	0.61	0.72	2.09	3.06	255.3	158.8
	2	64.8	47.1	9.9	19.3	16.7	13.2	8.6	20.4	1.6	0.7	0.5	1	4.21	3.01	0.63	0.73	2.11	3.05	231.5	129.6
	4	62.6	45.8	8.1	20.1	18.8	12.1	10.5	22.0	1.3	0.6	0.4	0.9	4.24	2.86	0.69	0.74	2.32	3.09	201.6	115.7
	6	60.2	42.2	9.3	23.2	17.6	11.8	12.9	22.8	1.1	0.7	0.6	0.8	4.01	2.41	0.71	0.78	2.27	3.11	168.2	114.2
	8	48.8	41.9	16.1	22.8	19.8	12.8	15.3	22.5	1.1	0.4	0.4	0.8	3.89	2.62	0.73	0.76	2.14	3.16	155.7	109.8
	S	53.6	38.2	15.8	23.6	13.8	16.1	16.8	22.1	32.5	21.3	15.4	24.1	4.18	2.97	0.62	0.68	2.13	2.25	171.2	121.8
XJ3	0	61.2	61.2	4.1	5.1	23.8	21.6	10.8	15.0	1.7	1.5	0.1	0.2	7.29	6.89	0.26	0.29	1.18	1.61	311.2	278.5
	2	61.6	58.9	5.3	5.4	22.6	20.8	10.5	14.9	1.7	1.5	0.1	0.2	7.31	6.88	0.26	0.27	1.13	1.65	289.6	267.3
	4	60.8	58.3	6.8	6.4	23.1	19.5	9.3	15.8	1.6	1.3	0.1	0.3	7.11	6.51	0.23	0.22	1.23	1.71	257.1	254.9
	6	60.1	57.2	6.5	7.6	23.8	17.6	9.6	17.6	1.5	1.5	0.2	0.2	7.01	6.37	0.21	0.31	1.18	1.66	261	239.1
	8	58.2	56.9	7.9	8.9	24.1	22.1	9.8	12.1	1.4	1.1	0.1	0.2	6.99	6.68	0.28	0.23	1.14	1.58	245.8	211.3
	S*																				
XJ4	0	65.4	55.6	3.8	14.7	19.2	15.2	11.6	14.5	0.9	0.6	0.2	0.6	3.9	3.01	0.47	0.51	2.92	4.03	216.3	156.6
	2	61.3	57.3	4.3	12.6	22.2	14.9	12.2	15.2	0.9	0.6	0.2	0.6	3.81	2.89	0.45	0.55	2.95	3.77	215.8	138.9
	4	58.2	51.9	7.7	16.2	15.3	16.6	18.8	15.3	0.8	0.5	0.3	0.6	3.63	2.71	0.51	0.52	2.91	3.62	208.1	166.8
	6	51.6	45.8	9.3	21.1	19.8	18.2	19.3	14.9	0.8	0.6	0.5	0.5	4.01	2.77	0.46	0.46	2.87	3.78	201.6	127.5
	8	42.1	38.9	8.8	24.6	24.5	20.2	24.6	16.3	0.7	0.4	0.3	0.4	3.87	2.58	0.45	0.48	2.61	4.11	186.2	132.9
	S	45.3	40.6	11.9	21.9	21.0	19.3	21.8	18.2	142.7	116.2	24.5	22.1	6.43	6.12	0.46	0.55	2.77	3.87	267.9	251.5
XJ6	0	58.6	53.3	12.2	15.2	15.6	8.5	13.6	23.0	1.3	0.6	0.3	0.5	1.99	1.58	0.51	0.62	2.33	2.8	68	50.1
	2	56.2	48.6	12.9	17.8	15.1	9.9	15.8	23.7	1.3	0.5	0.4	0.5	2.01	1.49	0.55	0.66	2.35	2.76	63.2	46.3
	4	48.7	46.9	13.6	18.4	20.5	8.6	17.2	26.1	1.2	0.4	0.2	0.3	1.96	1.38	0.57	0.73	2.41	2.84	56.9	45.1
	6	42.1	40.2	14.1	17.3	24.5	14.4	19.3	28.1	1.1	0.3	0.3	0.4	1.86	1.39	0.62	0.81	2.26	2.66	60.1	41.6
	8	39.8	36.5	14.3	19.8	24.4	18.2	21.5	25.5	0.9	0.5	0.3	0.4	1.73	1.42	0.63	0.73	2.18	2.51	45.6	39.5
	S	46.9	45.2	15.5	19.0	19.8	14.7	17.8	21.1	86.3	72.1	31.3	46.8	2.05	1.65	0.54	0.66	2.17	2.89	167.3	105.2
BJ	0	72.5	68.2	6.4	10.2	11.7	11.3	9.5	10.3	0.9	0.5	0.4	0.5	0.89	0.93	0.68	0.75	4.71	5.06	88.8	68.3
	2	65.6	67.2	8.7	11.5	14.5	9.8	11.2	11.5	0.9	0.5	0.4	0.4	0.87	0.92	0.69	0.73	4.71	5.01	86.4	66.2
	4	66.7	66.1	8.4	12.6	11.4	9.0	13.5	12.3	0.8	0.6	0.7	0.4	0.91	0.96	0.68	0.78	4.74	4.71	82.1	61.8
	6	68.2	64.2	6.2	13.1	13.8	10.8	11.8	11.9	0.5	0.4	0.3	0.6	0.84	0.91	0.66	0.81	4.81	4.75	78.9	55.6
	8	63.5	63.8	11.3	14.1	12.9	9.3	12.3	12.8	0.7	0.7	0.5	0.4	0.91	0.89	0.71	0.63	4.55	4.68	68.1	46.3
	S	62.8	61.3	8.8	15.1	15.2	12.0	13.2	11.6	25.1	19.8	13.8	22.9	0.93	0.81	0.65	0.68	4.36	4.71	31.6	26.7
DJ	0	63.9	53.6	10.1	16.0	9.9	10.1	16.0	20.5	0.3	0.4	0.4	0.6	1.11	1.21	0.72	0.81	3.16	4.88	45.2	39.8
	2	62.5	52.5	8.9	14.1	11.3	11.7	17.3	21.7	0.3	0.2	0.4	0.5	1.12	1.14	0.72	0.75	3.17	4.89	46.7	38.1
	4	62.1	51.3	9.2	11.9	10.5	13.2	18.2	23.6	0.2	0.3	0.3	0.4	1.05	1.12	0.73	0.79	3.22	4.85	44.2	36.3
	6	60.1	52.9	9.9	13.5	12.8	11.5	17.2	22.1	0.4	0.4	0.3	0.6	1.03	1.15	0.77	0.74	3.19	4.66	42.8	37.8
	8	58.9	52.7	11.0	9.9	13.2	12.8	16.9	24.6	0.4	0.3	0.3	0.5	1.02	1.04	0.72	0.73	3.12	4.81	43.6	39.6
	S	63.7	55.8	8.3	7.6	12.2	14.1	15.8	22.5	21.4	16.2	16.9	24.8	0.85	0.99	0.74	0.89	3.64	4.53	41.2	36.1

Sediment at XJ3 was not collected.

(1) Fatty acids

Similar to those from the surface water, water column samples from XJ3 contained the highest TFA value, with concentrations that ranged from 363.2 μg/L to 451.6 μg/L. There was little vertical change because XJ3 was characterized by low flow speed (a lacustrine condition). Hence, the fluctuation was weak. By contrast, XJ2 and XJ6 showed intense flood erosion features, leading to higher concentration at the surface. In addition, the water levels at these sites were low; intense erosion can result in the resuspension of the bottom sediment and vertical change.

Straight saturated fatty acids (SSFA) were the major FA fraction in the water column with values from 39.8 to 72.5% (winter) and from 36.5 to 68.2% (summer) of the total FAs. This showed a dominant aspect of aquatic OC input. Branched saturated fatty acids (BSFA) and PUFA exhibited lower contributions with values ranging from 12 to 22% and from 21 to 26% of the total FAs, respectively.

(2) Sterols

Sterol distribution in water column was dominated by $28^{\Delta5,22}$, $27^{\Delta5}$ (representing an aquatic autochthonous organic source), and $28^{\Delta5}$, $29^{\Delta5,22}$ (representing a terrigenous allochthonous organic source). The concentration of $28^{\Delta5,22}$ ranged from 0.2 to 1.7 mg/L in water column and 16.2 to 142.7 mg/kg in sediment. The highest and lowest value also appeared at XJ4 and DJ, respectively. In contrast, 29Δ5 was mainly detected at XJ6 with the highest value of 46.8 mg/kg in summer, revealing increasing input of terrestrial plant detritus caused by intense flood erosion. The ratio of $27^{\Delta5}/29^{\Delta5,22}+29^{\Delta5}$ was positively correlated with the input of the autochthonous OC source, and the results also showed that values in winter were higher than in summer.

(3) n-Alkanes

The results of the n-alkanes fraction in the water column and surface sediments in the Pearl River showed a wide distribution range of quantifiable n-C12 to n-C35 alkanes, which revealed a mixed aquatic and terrestrial source. Algal and photosynthetic products were generally characterized by low, odd-numbered carbon n-alkanes (n-C17), which were predominant in the Pearl River water and sediments. Similarly, the long-chain homologues (n-C27, n-C29, n-C31) derived from terrestrial higher plant waxes and the mid-chain n-alkanes of odd number (n-C23, n-C25) derived from lower plants were mainly detected in summer. Other n-alkane parameters such as TAR$_{H}$ ranged from 0.21 to 0.78 (average 0.59) in water column and from 0.46 to 0.89 (average 0.65). The lowest value appeared at XJ3 (0.21 in winter and 0.22 in summer), when the flow was slow and photosynthesis was intense, resulting in the accumulation of autochthonous OC.

In summary, sites with intense flood erosion character, for example XJ2 and XJ6, demonstrated vertical variation because of the complex process in terms of flood erosion and photosynthesis on the surface and resuspended sediments at the bottom. First, the sun supplied the energy for photosynthesis, which enhanced the surface synthesis of autochthonous OC, and values at all stations were higher than the bottom. Second, flood erosion carried terrestrial plant detritus into the river and resulted in increasing allochthonous OC. In contrast, in samples from the XJ3, BJ and DJ, the distribution of lipid biomarkers showed little variation from the surface to the bottom because of their weak flow character.

3.2.2. Grain-size distribution and its influence on the BCP effects

The grain size of suspended sediment can offer reflect the vertical transportation of suspended sediment[50]. Available data demonstrate considerable variation in the particle size characteristics of sediment from different sites in response to variations in source material and other physiographic controls [51].

We analyzed the vertical distribution of suspended sediments (0, 2, 4, 6, and 8 m from the water surface) and the surface sediments at the six stations (Table 4 and Figure 5). It is clear that a river with high flow speed can cause various mixing of grain size with characteristic coarse sand. XJ2, for example, was at the main steam of the Xijiang River and exhibited obvious river erosion features, with the d(0.5) (median grain size) value ranging from 101.16 to 157.07 μm in winter and 128.33 to 165.21 μm in summer. On the other hand, the water flow at XJ3 was relatively slow, resulting in the accumulation of fine sand. The grain size at XJ3 ranged from 6.07 to 7.61 μm in winter and 7.61 to 7.89 μm in summer. By taking the seasonal influence into account, summer usually had more precipitation that caused intense flood erosion, and thus the grain size was bigger in summer than in winter. This phenomenon was quite obvious at XJ2, XJ4 and XJ6, which were characterized by high flow rate, resulting in more coarse sand and a tremendous seasonal difference between winter and summer. In contract, XJ3, BJ and DJ had low flow velocity, therefore, the sediments were mainly composed by fine sand, and the seasonal difference was not so obvious. In addition, by comparing XJ1 and XJ3, it is clear that intense erosion also generated the resuspension of surface sediment and showed a bottom value higher than the surface water. Within the XJ3 section, the whole vertical grain size was quite small and almost the same, reflecting lacustrine feature.

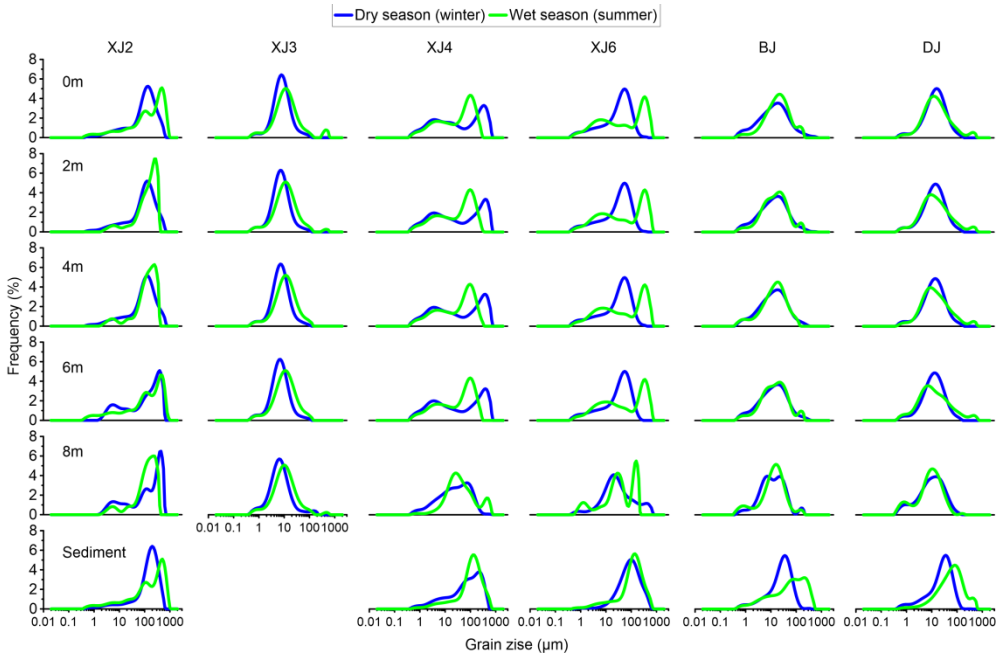


Figure 5. Grain size distribution of suspended particle and surface sediment.

Table 4. Seasonal comparison of chemical parameters of water column at various sites in Pearl River.

Site	Depth (m)	d(0.5) (μm)		DO (mg/L)		pH		EC (μs/cm)		T (℃)	
		winter	summer	winter	summer	winter	summer	winter	summer	winter	summer
XJ2	0	108.58	165.21	9.77	7.60	8.34	8.08	381	428	18.1	23.4
	2	102.58	150.26	9.14	8.41	7.99	8.06	313	435	17.8	23.6
	4	101.16	132.66	9.05	8.22	7.96	8.01	311	431	17.8	21.3
	6	131.36	129.63	8.92	7.69	7.89	7.90	309	425	17.8	23.9
	8	157.07	128.33	8.76	7.41	7.80	7.82	306	418	17.6	23.8
XJ3	0	7.61	11.35	7.89	10.27	7.57	8.56	381	320	18.4	28.9
	2	6.93	10.78	7.61	11.98	7.93	8.58	402	329	18.6	28.3
	4	6.86	10.77	7.69	9.54	7.88	8.57	382	322	18.1	27.9
	6	6.35	10.27	7.87	8.16	7.87	8.16	383	326	18.0	26.6
	8	6.07	9.46	7.86	8.03	7.88	8.02	381	329	18.0	26.7
XJ4	0	29.62	42.22	8.83	7.92	7.97	7.79	350	336	18.6	25.7
	2	29.38	41.52	8.98	7.61	7.95	7.86	353	335	18.6	26.3
	4	29.20	41.42	8.62	7.67	7.95	7.78	349	337	18.7	25.8
	6	28.48	40.98	8.55	7.33	7.94	7.83	348	336	18.6	26.0
	8	24.26	33.38	8.61	7.30	7.58	7.89	349	336	18.7	26.5
XJ6	0	36.08	49.02	8.70	6.77	7.76	7.63	310	227	17.9	28.0
	2	35.56	48.22	8.75	6.46	7.80	7.88	312	172.4	17.8	28.6
	4	35.42	47.05	8.73	6.80	7.79	7.85	312	174.7	17.8	28.7
	6	35.20	44.15	8.71	6.99	7.79	7.86	312	167.4	17.6	28.9
	8	23.91	31.07	8.70	6.93	7.78	7.81	312	167.9	17.6	29.1
BJ	0	13.37	18.59	9.54	5.72	7.63	7.07	237	96.2	15.6	29.2
	2	12.82	14.25	10.37	5.65	7.89	7.54	241	96.6	15.0	29.8
	4	12.70	13.85	10.27	5.54	7.87	7.69	239	93.6	14.8	31.5
	6	12.43	13.69	10.33	5.19	7.85	7.33	240	94.0	14.8	30.0
	8	10.83	12.69	10.33	4.54	7.92	7.47	240	104.6	14.9	28.6
DJ	0	13.78	13.69	9.00	6.01	7.12	7.52	135	172.6	17.5	28.3
	2	12.39	12.10	9.36	6.26	7.15	7.63	138	171.8	17.5	29.8
	4	11.99	12.08	9.28	5.79	7.34	7.58	136	168.1	17.1	29.6

6	11.48	10.27	9.23	5.75	7.48	7.52	136	174.4	17.1	28.7
8	9.73	8.737	9.15	5.70	7.43	7.48	135	170.6	17.3	29.4

d(0.5): median grain size

Figure 6 demonstrates that the main mechanism of vertical transportation during the BCP process was derived by the adsorption of clay material, which allowed the formed OC at the surface area to vertically move to the bottom and finally be stored as sediment. Hence, when estimating the carbon sink in the aquatic system, OC buried in the sediment must be taken into account.

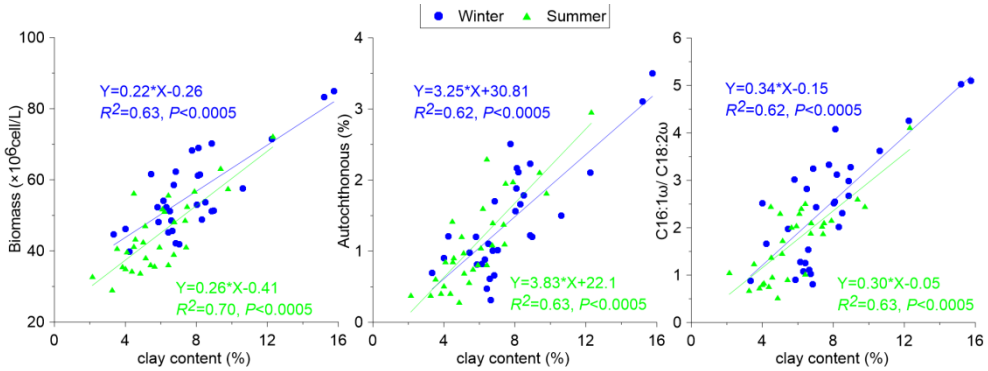


Figure 6. Relationship between photosynthesis and sediment grain size.

3.3. Carbon sink estimation based on the photosynthesis-coupled-carbonate-weathering

Source identification of organic carbon in the Pearl River is very difficult because of the mixed effects of rock weathering, photosynthesis, and stream erosion. Lipid biomarkers can provide unique bio-information and are extensively used to distinguish autochthonous and allochthonous OCs. The ratio of autochthonous and allochthonous OCs represents the in situ productivity of the aquatic system over allochthonous input.

The results showed that the autochthonous organic source in surface water of the Pearl River was the predominant input with averages of 65% and 54% in winter and summer, respectively (Figure 7). This value in water column was 55.9% (winter) and 44.6% (summer), in surface sediment 52.1% (winter) and 43.9% (summer) (Figure 8). The results indicated that autochthonous OC in the aquatic system was mainly derived from the in situ primary productivity.

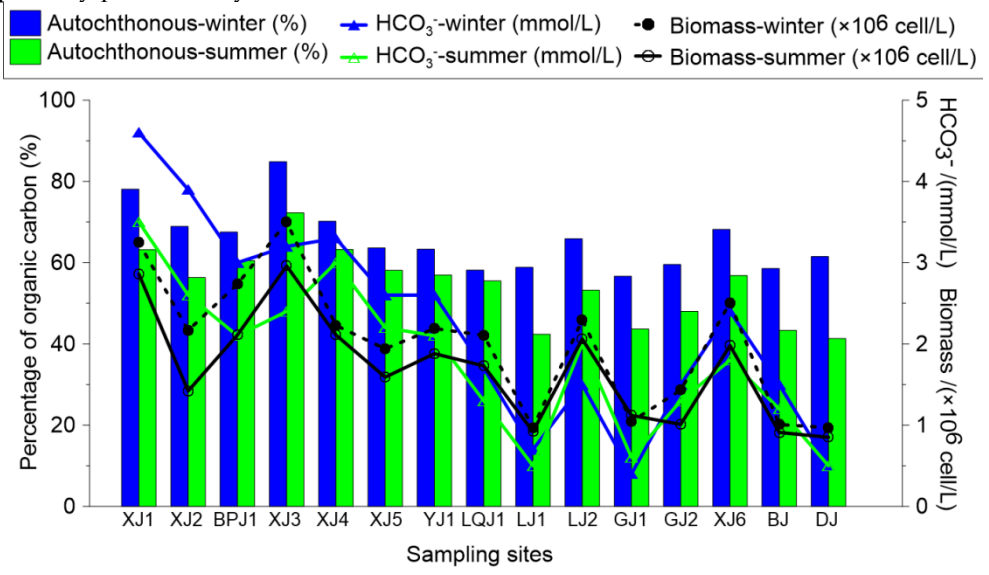


Figure 7. Seasonal and spatial distributions of autochthonous(%) and allochthonous(%) OC and the hydrochemical (HCO_3^-) and biological (C16:1ω/C18:2ω and biomass) parameters;

TAR_{FA}=(C24+C26+C28)/(C12+C14+C16); Autochthonous(%)=ΣSCFA(C12~C18)/TAR_{FA}; Allochthonous (%)=ΣLCFA(C22~C30)/TAR_{FA}).

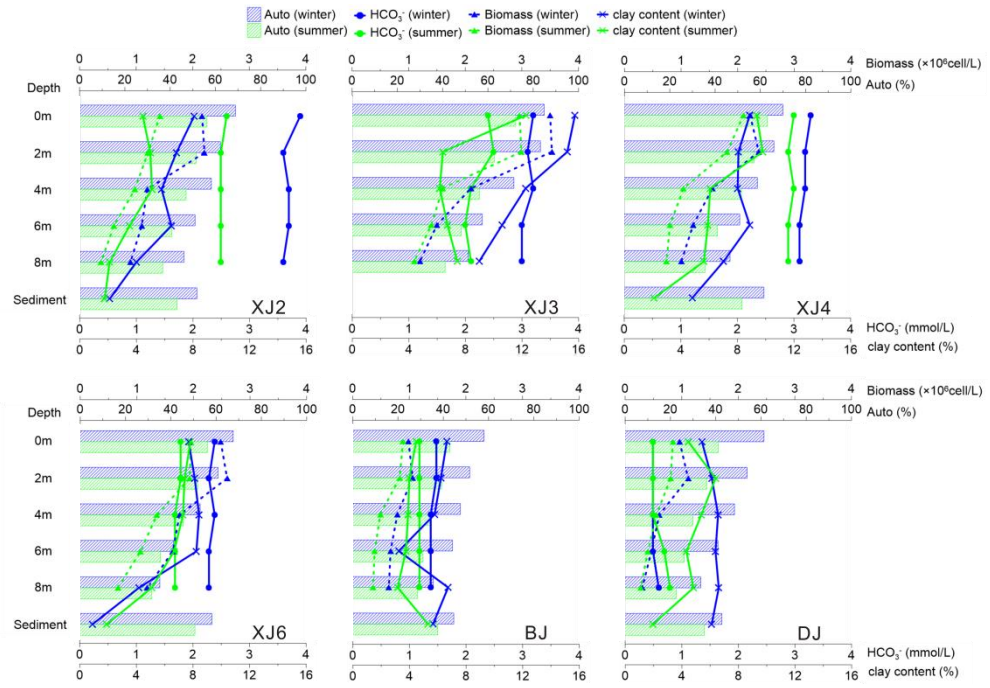


Figure 8. Vertical variation of autochthonous ratio of organic carbon and relevant biogeochemical indexes in water column and surface sediments of Pearl River.

It is obvious that due to the BCP effects, OC derived from the aquatic photosynthetic use of carbonate-weathering derived DIC was vertically transported through the adsorption by clay material and finally stored in the sediment. According to the rock-weathering related carbon sink model, the pure karst carbon sink in the riverine system could be calculated by the equation showing below [12]. $CSF=Q_{water}\times(DIC/2+TOC_{water}\times Auto\%_{water})+F_{sediment}\times TOC_{sediment}\times Auto\%_{sediment}$, where the Q_{water}, $F_{sediment}$, TOC_{water}, $TOC_{sediment}$, $Auto\%_{water}$ and $Auto\%_{sediment}$ represent the flow rate, sediment flux, and TOC concentration in water and sediment, and the ratio of autochthonous to TOC in water and sediment, respectively. Wei et al. reported that the average annual TOC concentration in the Pearl River was 4.71 mg/L, and the DIC concentration was 11.17 mg/L [52]. The average concentration of TOC in sediment was 1.1% dry wet (or 11000 mg/kg) and the annual flow rate 283×10^9 m^3, and the sediment flux 72.4×10^6 t (Ministry of Water Resource, PRC, 1954-2010) [38].

By taking the average value of the autochthonous ratio to TOC in both the water column and surface sediments in the Pearl River, and using the above values, we estimated that the karst carbon sink in the Pearl River was 2.69×10^6 t/a, which was 1.7 times traditional estimation ($CSF=Q\times DIC/2=1.58\times10^6$ t/a). Hence, the contribution of the riverine ecosystem to global karst carbon sink may have a larger potential than we ever thought, which didn't consider the BCP effect.

4. Conclusion

The present study examines the lipid biomarker and biochemical composition in both the water column and surface sediments of the Pearl River collected along the river and at six depth profiles in winter (dry season, January to February) and summer (wet season, July to August). In addition, the full range of sediment grain sizes were also determined to reveal the mechanism of BCP effects in the riverine system and estimate the autochthonous OC and their contribution to carbon sink. The results exhibited the following: (1)

both the concentrations of OC and biochemical compositions showed significant spatial and seasonal variations, which are the combined results of the processes of aquatic photosynthesis, carbonate weathering, flood erosion, particle adsorption and suspended sediment deposition. More specifically, sites with high DIC concentrations offer a continuous carbon source for photosynthetic activity and increase the amount of autochthonous source, resulting in a high autochthonous OC ratio. Summer usually has intense precipitation and flood erosion that dilutes the biogeochemical composition and carries terrestrial plant detritus; therefore, the auto% value was higher in winter than in summer. According to the calculation of lipid biomarkers, the auto% values were 65% (winter), 54% (summer) in surface water, 55.9% (winter) and 44.6% (summer) in water column and 52.1% (winter) and 43.9% (summer) in surface sediment, which demonstrated autochthonous OC accounted for a main part of the TOC. (2) Vertical variability mainly appeared at sites with intense flood erosion characteristics. There is a positive correlation between clay content and the auto% value and the biogeochemical composition, reflecting that clay adsorbed organic carbon in the water and vertically deposited into the sediment was the dominant mechanism of vertical delivery of OC. (3) According to the new carbon sink model based on coupled carbonate weathering with aquatic photosynthesis, the karst carbon sink flux (CSF) in the Pearl River was 2.69×10^6 t/a, which was 1.7 times traditional estimation (1.58×10^6 t/a), which didn't consider the BCP effect, revealing that the contribution of the riverine ecosystem to the global carbon sink may have larger potential than we ever thought. These results may offer direction to seek the global missing carbon sink.

Author Contributions: Conceptualization, Z.L.; methodology, M.Y.; software, M.Z.; formal analysis, M.Y.; investigation, M.Y. and H.S.; data curation, M.Y. and H.S.; writing—original draft preparation, W.Y.; writing—review and editing, M.Y. and Z.L.; visualization, H.H.; supervision, Z.L. All authors have read and agreed to the published version of the manuscript.

Funding: This research was sponsored by the Projects of National Natural Science Foundation of China [No. U1612441, 41602275, 41977298]; Guizhou Provincial Science and Technology Projects [QKHJC-ZK(2022)-General 186], the talents project of Guizhou technology platform ([2017] 5789-17).

Institutional Review Board Statement: Not applicable.

Informed Consent Statement: Not applicable.

Data Availability Statement: Not applicable.

Conflicts of Interest: The authors declare no conflict of interest.

References

1. Rixen, T., Goyet, C., Ittekkot, V. Diatoms and their influence on the biologically mediated uptake of atmospheric CO_2 in the Arabian Sea upwelling system. *Biogeosciences* **2006**, *3(1)*, 1–13.
2. Goodwin, P., Lauderdale, J.M. Carbonate ion concentrations, ocean carbon storage, and atmospheric CO_2. *Glob. Biogeochem. Cy.* **2013**, *27(3)*, 882–893.
3. Sun, H.G., Han, J.T., Zhang, S.R., Lu, X.X. Transformation of dissolved inorganic carbon (DIC) into particulate organic carbon (POC) in the lower Xijiang River, SE China, an isotopic approach. *Biogeosci. Discuss*. **2011**, *8(5)*, 9471–9501.
4. Liu, Z. Review on the role of terrestrial aquatic photosynthesis in the global carbon cycle. *Proc. Earth Planet. Sci.* **2013**, *7(3–4)*, 513–516.
5. Romera-Castillo, C., Álvarez-Salgado, X.A., Galí, M., Gasol, J.M., Marrase, C. Combined effect of light exposure and microbial activity on distinct dissolved organic matter pools. A seasonal field study in an oligotrophic coastal system (Blanes Bay, NW Mediterranean). *Mar. Chem.* **2013**, *148(2)*, 44–51.
6. Yang, R., Chen, B., Liu, H., Liu, Z., Yan, H. Carbon sequestration and decreased CO2, emission caused by terrestrial aquatic photosynthesis: Insights from diel hydrochemical variations in an epikarst spring and two spring-fed ponds in different seasons. *Appl. Geochem*. **2015**, *63(3)*, 248–260.
7. Medeiros, P.M., Simoneit, B.R.T. Multi-biomarker characterization of sedimentary organic carbon in small rivers draining the Northwestern United States. *Org. Geochem*. **2008**, *39(1)*, 52–74.

8. Matsunaga, K. An estimation of allochthonous and autochthonous organic matter of the fresh sediments on the basis of Ti content. *Jap. J. Limnol*. **2009**, *43(2)*, 113–120.
9. Waterson, E.J., Canuel, E.A. Sources of sedimentary organic matter in the Mississippi River and adjacent Gulf of Mexico as revealed by lipid biomarker and $\delta^{13}C_{TOC}$ analyses. *Org. Geochem*. **2008**, *39(4)*, 422–439.
10. Yang, M., Liu, Z., Sun, H., Yang, R., Chen, B. Organic carbon source tracing and DIC fertilization effect in the Pearl River: insights from lipid biomarker and geochemical analysis. *Appl. Geochem*. **2016**, *73*, 132–141.
11. Bianchi, T.S. *Biogeochemistry of estuaries*. Oxford University Press, New York, USA, 2007.
12. Liu, Z., Dreybrodt, W. Significance of the carbon sink produced by H2O-carbonate-CO2-aquatic phototroph interaction on land. *Sci. Bull*. **2015**, *60(2)*, 182–191.
13. Liu, Z., Macpherson, G.L., Groves, C., Martin, J.B., Yuan, D.X., Zeng, S. Large and active CO2, uptake by coupled carbonate weathering. *Earth-Sci. Rev.* **2018**, *182*, 42–49.
14. Goni, M.A., Monacci, N., Gisewhite, R., Ogston, A., Crockett, J., Nittrouer, C. Distribution and sources of particulate organic matter in the water column and sediments of the Fly River Delta, Gulf of Papua (Papua New Guinea). *Estuar. Coast. Shelf Sci*. **2006**, *69(1–2)*, 225–245.
15. Battin, T.J., Kaplan, L.A., Findlay, S., Hopkinson, C.S., Marti, E., Packman, A.I., Newbold, J.D., Sabater, F. Biophysical controls on organic carbon fluxes in fluvial networks. *Nature Geosci*. **2009**, *1(8)*, 95–100.
16. Aufdenkampe, A.K., Mayorga, E., Raymond, P.A,, Melack, J.M., Doney, S.C., Alin, S.R., Aalto, R.E., Yoo, K. Riverine coupling of biogeochemical cycles between land, oceans, and atmosphere. *Front. Ecol. Environ*. **2011**, *9(1)*, 53–60.
17. Tao, S., Eglinton, T.I., Montluçon, D.B., Mcintyre, C., Zhao, M. Pre-aged soil organic carbon as a major component of the Yellow River suspended load: Regional significance and global relevance. *Earth Planet. Sci. Lett*. **2015**, *414*, 77–86.
18. Mayer, L.M. Extent of coverage of mineral surfaces by organic matter in marine sediments. *Geochim. Cosmochim. Acta*. **1999**, *63(2)*, 207–215.
19. Keil, R.G., Mayer, L.M., Quay, P.D., Richey, J.E., Hedges, J.I. Loss of organic matter from riverine particles in deltas. *Geochim. Cosmochim. Acta*. **1997**, *61(7)*, 1507–1511.
20. Ransom, B., Kim, D., Kastner, M., Wainwright, S. Organic matter preservation on continental slopes: importance of mineralogy and surface area. *Geochim. Cosmochim. Acta*. **1998**, *62(8)*, 1329–1345.
21. Bock, M.J., Mayer, L.M. Mesodensity organo-clay associations in a near-shore sediment. *Mar. Geol*. **2000**, *163(1)*, 65–75.
22. Curry, K.J., Bennett, R.H., Mayer, L.M., Curry, A., Abrli, M., Biesiot, P.M., Hulbert, M.H. Direct visualization of clay microfabric signatures driving organic matter preservation in fine-grained sediment. *Geochim. Cosmochim. Acta*. **2007**, *71(7)*, 1709–1720.
23. Galy, V., France–Lanord, C., Lartiges, B. Loading and fate of particulate organic carbon from the Himalaya to the Ganga–Brahmaputra delta. *Geochim. Cosmochim. Acta*. **2008**, *72(7)*, 1767–1787.
24. West, A.J., Lin, C.W., Lin, T.C., Hilton, R.G., Liu, S.H., Chang, C.T., Lin, K.C., Galy, A., Sparkes, R.B., Hovius, N. Mobilization and transport of coarse woody debris to the oceans triggered by an extreme tropical storm. *Limnol. Oceanogr*. **2011**, *56(1)*, 77–85.
25. Guschina, I.A., Harwood, J.L. *Algal Lipids and Their Metabolism. Algae for Biofuels and Energy*, Springer, Netherlands, 2013..
26. Mohanty, B.P., Bhattacharjee, S., Paria, P., Mahanty, A., Sharma, A.P. Lipid biomarkers of lens aging. *Appl. Biochem. Biotech*. **2013**, *169*, 192–200.
27. Eglinton, G., Hamilton, R.J. Leaf epicuticular waxes. *Science* **1967**, *156*, 1322–1335.
28. Robinson, N., Cranwell, P. A., Eglinton, G. Sources of the lipids in the bottom sediments of an English oligo-mesotrophic lake. *Freshwater Biol*. **1987**, *17*, 15–33.
29. Gao, L., Hou, J., Toney, J., Macdonald, D., Huang, Y. Mathematical modeling of the aquatic macrophyte inputs of mid-chain n-alkyl lipids to lake sediments: Implications for interpreting compound specific hydrogen isotopic records. *Geochim. Cosmochim. Acta*. **2011**, *75(13)*, 3781–3791.
30. Dunstan, G.A., Volkman, J.K., Barrett, S.M., Leroi, J.M., Jeffrey, S.W. Essential polyunsaturated fatty acids from 14 species of diatom (Bacillariophycea). *Phytochemistry* **1993**, *35*, 155–161.
31. Harwood, J.L., Russell, N.J. *Lipids in Plants and Microbes*. George Allen and Unwin, London, British, 1984.
32. Volkman, J.K. A review of sterol markers for marine and terrigenous organic matter. *Org. Geochem*. **1986**, *9*, 83–99.
33. Yunker, M.B., MacDonald, R.W., Veltkamp, D.J., Cretney, W.J. Terrestrial and marine biomarkers in a seasonally ice-covered Arctic estuary-integration of multivariate and biomarker approaches. *Mar. Chem*. **1995**, *49*, 1–50.
34. Tue, N.T., Quy, T.D., Hamaoka, H., Mai, T.N., Omori, K. Sources and exchange of particulate organic matter in an estuarine mangrove ecosystem of Xuan Thuy National Park, *Vietnam. Estuar. Coasts*. **2012**, *35*, 1060–1068.
35. Zhang, S.R., Lu, X.X., Higgitt, D.L., Chen, C.T.A., Han, J.T., Sun, H.G. Recent changes of water discharge and sediment load in the Zhujiang (Pearl River) basin, China. *Glob. Planet. Change* **2008**, *60*, 365–380.
36. Sun, H.G., Han, J., Li, D., Zhang, S.R., Lu, X.X. Chemical weathering inferred from riverine water chemistry in the lower Xijiang basin, South China. *Sci. Total Environ*. **2010**, *408*, 4749–4760.
37. Zhang, Q., Xu, C., Gemmer, M., Chen, Y., Liu, C. Changing properties of precipitation concentration in the Pearl River basin, China. Stochast. Environ. *Res. Risk Assess*. **2009**, *23 (3)*, 377–385.
38. Ministry of Water Resource, P.R.C., 1954–2010. *China River Sediment Bulletin*. China Water Power Press, Beijing, China, 2011. (in Chinese)
39. He, L., Yang, Q., Ou, S. Temporal variation of runoff and sediment on the main channels of Xijiang River and Beijiang River. *Guangdong Water Res. Hydropower*. **2003**, *1*, 57–62 . (in Chinese)

40. Cheng, Y.Q. *Geological atlas of China (1: 5,000,000)*. China Cartographic Pressing House, Beijing, China, 1990. (in Chinese)
41. Liu, Z., Li, Q., Sun, H., Wang, J. Seasonal, diurnal and storm-scale hydrochemical variations of typical epikarst springs in subtropical karst areas of SW China, Soil CO2 and dilution effects. *J. Hydrol*. **2007**, *337*, 207–223.
42. Wigley, T. WATSPEC, a computer program for determining the equilibrium speciation of aqueous solutions. Brit. Geomorphol. *Res. Group Tech., Bull*. **1977**, *20*, 1–48.
43. MEP, Ministry of Environmental Protection of the People's Republic of China. Monitoring and Analysis Method of Water and Waste Water, Environmental Science Press (4th edition), Beijing, China, 2002.
44. Mortillaro, J.M., Abril, G., Moreira-Turcq, P., Sobrinho, R.L., Perez, M., Meziane, T. Fatty acid and stable isotope (δ13C, δ15N) signatures of particulate organic matter in the lower Amazon River: Seasonal contrasts and connectivity between floodplain lakes and the mainstem. *Org. Geochem*. **2011**, *42*, 1159–1168.
45. Zheng, B., Zhou, J., Liu, L., Lin, K., Zhu, Y. The reference condition for Eutrophication Indictor in the Yangtze River Estuary and adjacent—waters response variables. *Acta Ecol. Sin*. **2013**. *33*. 2780–2789.
46. Dunstan, G.A., Volkman, J.K., Barrett, S.M., Garland, C.D. Changes in the lipid composition and maximisation of the polyunsaturated fatty acid content of three microalgae grown in mass culture. *J. Appl. Phycol*. **1993**, *5*, 71–83.
47. Viso, A.C., Marty, J.C. Fatty acids from 28 marine microalgae. *Phytochemistry* **1993**, *34*, 1521–1533.
48. Li, W., Dagaut, J., Saliot, A. The application of sterol biomarkers to the study of the sources of particulate organic matter in the Solo River system and Serayu River, Java, Indonesia. *Biogeochemistry* **1995**, *31*, 139–154.
49. Meyers, P.A. Organic geochemical proxies of paleoceanographic, paleolimnologic, and paieoclimatic processes. *Org. Geochem*. **1997**, *27*, 213–250.
50. Walling, D.E., Moorehead, P.W. Spatial and temporal variation of the particle-size characteristics of fluvial suspended sediment. *Geograf. Ann*. **1987**, *69(1)*, 47–59.
51. Walling, D.E., Moorehead, P.W. The particle size characteristics of fluvial suspended sediment, an overview. *Hydrobiologia* **1989**, *176–177(1)*, 125–149.
52. Wei, X., Shen, C., Li, D., Wu, Z.F., He, J.H., Zhu, L.A. The inventory and fluxes of carbon in soil of Pearl River basin. *Ecol. Environ*. **2004**. *13(4)*. 670–673. (in Chinese)